

Author Manuscript

Title: Mechanochemical Synthesis of Active Magnetite Nanoparticles Supported on Charcoal for Facile Synthesis of Alkynyl Selenides via C-H Activation

Authors: Balaji Mohan; Ji Chan Park; Kang Hyun Park, Ph.D.

This is the author manuscript accepted for publication and has undergone full peer review but has not been through the copyediting, typesetting, pagination and proofreading process, which may lead to differences between this version and the Version of Record.

To be cited as: 10.1002/cctc.201600280

Link to VoR: <http://dx.doi.org/10.1002/cctc.201600280>

Mechanochemical Synthesis of Active Magnetite Nanoparticles Supported on Charcoal for Facile Synthesis of Alkynyl Selenides via C-H Activation

Balaji Mohan^[a], Ji Chan Park^{*[b]} and Kang Hyun Park^{*[a]}

Abstract: Magnetite (Fe_3O_4) nanoparticles supported on (charcoal, graphene, or SBA-15) were prepared by a simple solid-state grinding technique and subsequent thermal treatment. The Fe_3O_4 nanoparticles supported on activated charcoal exhibited high catalytic activity furnishing a good product yield of alkynyl selenides in the cross-coupling reaction of diphenyl diselenides and alkynes through activation of C-H and Se-Se bonds under eco-friendly conditions, surpassing traditional copper based catalysts to effect the same organic transformation.

Transition metal nanoparticles (NPs) have recently been of scientific and technological interest in various areas such as sensors, fuel cells, homo and heterogeneous catalysts for important organic transformations.^[1] So far, a number of solid-supported transition metal nanoparticles, such as Cu, Au, Ru, Rh, Ir, Ni and Pd have been widely used as heterogeneous catalysts for important catalytic processes.^[2]

In particular, iron-oxide NPs have been widely used as solid supports for the purpose of stabilizing metal nanoparticles to avoid leaching, complete recovery using external magnetic field for recycling and also to circumvent contamination with target products.^[3] Despite, owing to low cost, naturally abundant and environmentally friendly material, recently, the use of iron-oxide NPs itself has been effectively utilized as catalysts for important organic reactions, such as, nitrophenol reduction, benzyl alcohol oxidation, sonogashira coupling, borylation, multicomponent synthesis and so on.^[4] By tuning the surface design of the support along with the size and shape of the nanoparticles, the hunt for



Scheme 1. A facile synthesis of $\text{Fe}_3\text{O}_4/\text{C}$ nanocatalysts by infiltration

and thermal treatment.

more suitable solid supports for Fe_3O_4 NPs to provide highly efficient, more recycles, and also to achieve target products at low- catalyst loading.

Considerable efforts have been made to fabricate Fe_3O_4 NPs on various supports. Traditionally, the preparation method of the catalyst included multiple steps such as preparation of nanoparticles, isolation, drying and followed by immobilization on suitable supports. However, in industry, the use of a simple method using low price supports is still needed, because a cost of supported catalyst preparation is important as well as activity and reusability of the catalyst. Therefore, a facile and economical technique without any pretreatment of solid supports is desired for a catalyst synthesis.

Recently, solid-state grinding with sequential infiltration of metal salts (i.e., melt-infiltration process) has been utilized as a convenient and fast route in order to prepare supported metal catalysts due to easy synthetic procedures, superior product crystallinity and ease of scaling up.^[5] Herein, we report an easy synthesis of iron-oxide NPs supported on activated charcoal ($\text{Fe}_3\text{O}_4/\text{C}$) by a facile and economic synthetic technique. In order to check and compare the high activity and stability of $\text{Fe}_3\text{O}_4/\text{C}$ catalyst in the catalytic reactions for alkynyl selenide compound synthesis, other well-known supports (graphene and SBA-15) are tested as a support. Figure 1 depicts photographs of Fe_3O_4 NPs supported on charcoal, graphene and SBA-15, respectively.



Figure 1. Pictorial representation of Fe_3O_4 NPs on charcoal, single-layer graphene, and SBA-15 from left to right.

[a] Dr. B. Mohan, Prof. K. H. Park
Department of Chemistry and Chemistry Institute for Functional Materials
Pusan National University, Busan 609-735 (Republic of Korea)
E-mail: chemistry@pusan.ac.kr

[b] Dr. J. C. Park,
Clean Fuel Laboratory,
Korea Institute of Energy Research, Daejeon 305-343
E-mail: jcpark@kier.re.kr
Supporting information for this article is given via a link at the end of the document.

Scheme 1 demonstrates the simple synthetic procedure for the $\text{Fe}_3\text{O}_4/\text{C}$ catalyst. First, $\text{Fe}(\text{NO}_3)_3 \cdot 9\text{H}_2\text{O}$ salt was melt-infiltrated into mesoporous charcoal powder by grinding at room temperature and subsequently aging at 50°C for 24 h in a tumbling oven. Then, small magnetite nanoparticles around

13 nm were obtained by thermal decomposition of the confined salt in carbon pores at 400°C under a nitrogen flow. The high-angle annular dark-field scanning transmission electron microscopy (HAADF-STEM) image shows bright dots which mean the incorporated Fe_3O_4 nanoparticles in the porous charcoal support (Figure 2a). The small Fe_3O_4 particles with an average diameter of 12.6 nm are observed (Figure 2b and 2d). High-resolution TEM (HRTEM) analysis revealed the lattice fringe images of the Fe_3O_4 particles, measured to be 0.253 nm of the (311) planes (Figure 2c). XRD (X-ray powder diffraction) spectrum were well-matched with the Fe_3O_4 phase (Figure 2e, JCPDS No. 19-0629). The average size of the Fe_3O_4 nanoparticles is estimated to be 13.0 nm from the broadness of the (111) peak by the Debye–Scherrer equation. N_2 sorption experiments at -196°C for the $\text{Fe}_3\text{O}_4/\text{C}$ exhibited type IV adsorption–desorption hysteresis with delayed capillary evaporation at a relative pressure of 0.5 (Figure 2f). The Brunauer–Emmett–Teller (BET) surface area and total pore volume of the $\text{Fe}_3\text{O}_4/\text{C}$ was calculated to be $642\text{ m}^2 \cdot \text{g}^{-1}$ and $0.48\text{ cm}^3 \cdot \text{g}^{-1}$, respectively. The size of the small pores of $\text{Fe}_3\text{O}_4/\text{C}$ was 3.9 nm, obtained from the desorption branches.

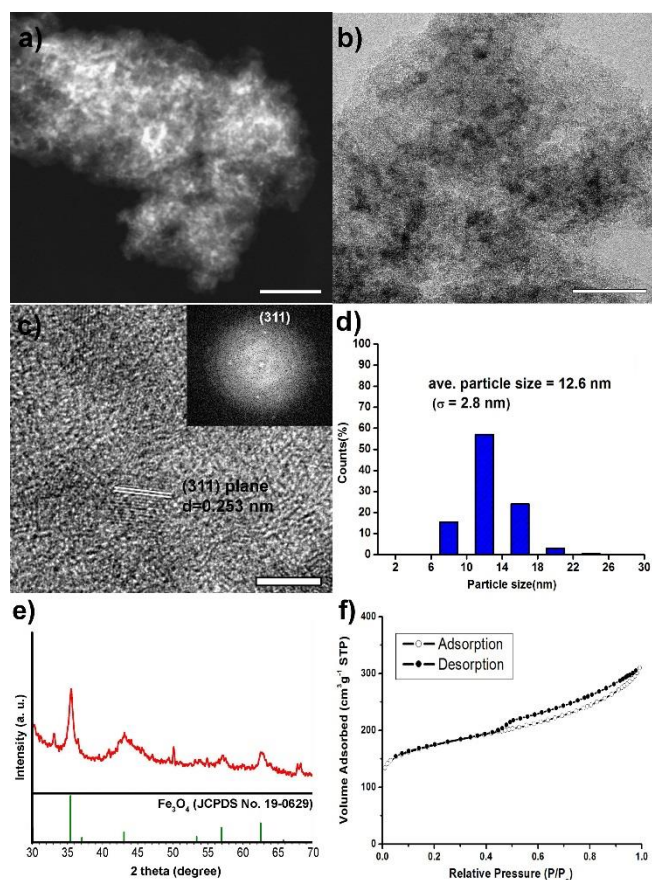


Figure 2 (a) HAADF, (b) low-resolution TEM, (c) high-resolution TEM images with corresponding FT pattern (inset of c), (d) particle size distribution histogram, (e) XRD spectrum, and (f) N_2 adsorption/desorption isotherms of $\text{Fe}_3\text{O}_4/\text{C}$ catalyst. More than 200 particles were counted for the sample. The bars represent 100 nm (a), 50 nm (b), and 5 nm (c).

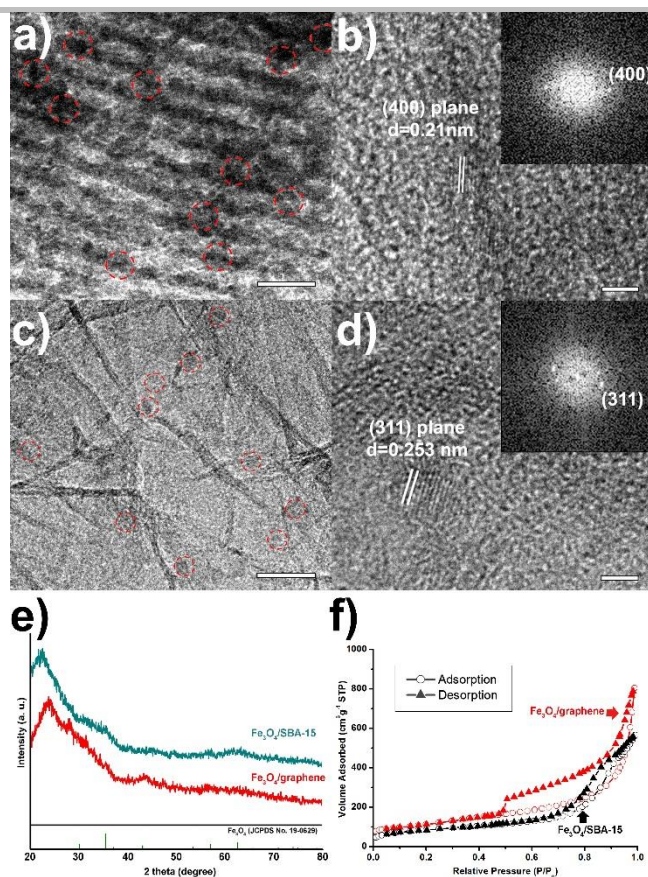


Figure 3 (a) TEM and (b) HRTEM images of $\text{Fe}_3\text{O}_4/\text{SBA-15}$ with corresponding FT pattern (inset of b), (c) TEM and (d) HRTEM images of $\text{Fe}_3\text{O}_4/\text{graphene}$ with corresponding FT pattern (inset of b), (e) XRD spectra, and (f) N_2 adsorption/desorption isotherms of $\text{Fe}_3\text{O}_4/\text{SBA-15}$ and $\text{Fe}_3\text{O}_4/\text{graphene}$. The bars represent 20 nm (a,c) and 2 nm (b,d). The red circles (a, c) indicate small nanoparticles.

In order to compare $\text{Fe}_3\text{O}_4/\text{C}$ catalyst with other supported Fe_3O_4 catalysts, $\text{Fe}_3\text{O}_4/\text{SBA-15}$ and $\text{Fe}_3\text{O}_4/\text{graphene}$ catalysts were introduced through the same procedures. The SBA-15 was chosen as a representative porous silica support with high surface area and regular pore structure. The $\text{Fe}_3\text{O}_4/\text{SBA-15}$ shows very small nanoparticles around 2 nm (Figure 3a). HRTEM analysis revealed the lattice fringe image of Fe_3O_4 phase, measured to be 0.21 nm of the (400) planes (Figure 3b). In $\text{Fe}_3\text{O}_4/\text{graphene}$ catalyst, the particle size was less than 2 nm, therefore not be easily monitored even at HRTEM images (Figure 3c). The red circles marked in Figure 3a and c indicate extremely small nanoparticles. The lattice fringe image of the Fe_3O_4 particles was measured to be 0.253 nm of the (311) planes (Figure 3d). Comparing peak intensities, the particle sizes of Fe_3O_4 in SBA-15 and graphene were much smaller than that of $\text{Fe}_3\text{O}_4/\text{C}$ catalyst (Figure 3e). The BET surface areas of $\text{Fe}_3\text{O}_4/\text{SBA-15}$ and $\text{Fe}_3\text{O}_4/\text{graphene}$ were calculated to be $303\text{ m}^2 \cdot \text{g}^{-1}$ and $394\text{ m}^2 \cdot \text{g}^{-1}$, respectively (Figure 3f). The total pore volumes of the $\text{Fe}_3\text{O}_4/\text{SBA-15}$ and $\text{Fe}_3\text{O}_4/\text{graphene}$ were $0.88\text{ cm}^3 \cdot \text{g}^{-1}$ and $1.24\text{ cm}^3 \cdot \text{g}^{-1}$, respectively. The Fe-loading content for all catalysts was calculated to be approximately 10 wt% on the basis of Fe converted from the iron nitrate salt after the thermal treatment.

The catalytic activity of synthesized Fe_3O_4 NPs has been tested in the cross-coupling reaction of diphenyl diselenide with

an alkyne to obtain corresponding alkynyl selenides *via* activation of C-H and Se-Se bonds.

The chemistry of organochalcogens, especially selenium, has been expanding rapidly over the last decade. There have been enormous effort has been devoted to develop novel organochalcogen compounds for potential applications in the field of modern organic synthesis and catalysis. Organoselenium compounds are particularly attractive and gained considerable attention among researchers, because of their ability to mimic natural compounds with important biological properties, like antiviral, antimicrobial, antitumor and antioxidant.^[6] Moreover, chalcogen derivatives have also been applied in the development of organic material, such as liquid crystals, organic semiconductors and electroconductive polymers.^[7] In this context, we have recently developed various synthetic procedures to obtain organochalcogen derivatives that used nanocatalysts. Taking into consideration our program devoted towards the synthesis of organochalcogen compounds, we turned our attention to alkynyl selenides.^[8, 2b]

The literature survey shows that various type of catalysts especially copper have been front-runner in order to make Csp-Se bond via a cross-coupling reaction of either terminal alkynes or alkynyl halides with a convenient source of electron-deficient selenium^[9, 8a] affording alkynyl selenides in high yields. Although, rather effective, these approaches suffers from several drawbacks: (1) the preparation of alkynyl halides, (2) require phosphine or nitrogen based ligands, (3) toxic solvents, (4) homogeneous process, (5) harsh reaction conditions, (5) environmental impact, which in some cases may increase the cost and limit the scope of the reaction.

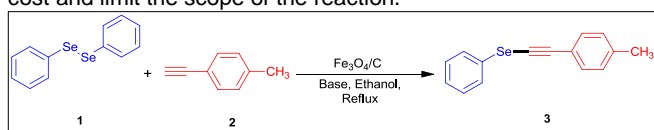


Table 1. Optimization of reaction conditions^[a]

Entry	Base	Catalyst	Yield % ^[b]
1	KO ^t Bu	-	19 ^[c]
2	KO^tBu	Fe₃O₄/C	81 (78)^[d]
3	K ₂ CO ₃	Fe ₃ O ₄ /C	59
4	KOH	Fe ₃ O ₄ /C	73
5	K ₃ PO ₄	Fe ₃ O ₄ /C	63
6	Na ₂ CO ₃	Fe ₃ O ₄ /C	2
7	Cs ₂ CO ₃	Fe ₃ O ₄ /C	64
8	KO ^t Bu	Fe ₃ O ₄ /C	71 ^[e]
9	KO ^t Bu	Fe ₃ O ₄ /SBA 15	61 ^[f]
10	KO ^t Bu	Fe ₃ O ₄ /Graphene	70 ^[g]

[a] Reaction conditions: **1** (1 mmol), **2** (2 mmol), base (2 mmol), catalyst (0.5 mol% respect to **1**) [b] Determined by GC-MS [c] In the absence of a catalyst, 24 h [d] Isolated yield [e] Reaction with 1 equiv of base [f] 0.5% Fe₃O₄/SBA-15 catalyst [g] 0.5% Fe₃O₄/graphene catalyst, 80°C, 12 h.

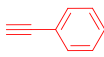
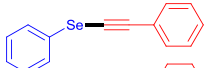
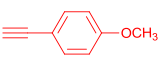
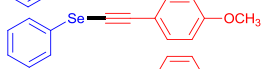
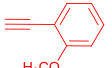
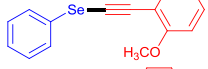
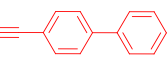
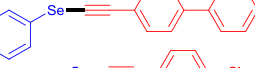
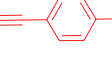
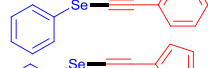
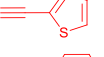
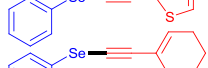

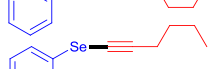

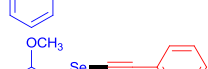
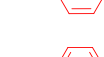
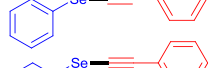
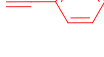

In addition, most of the reported synthetic techniques used either DMSO or DMF as solvent and as well as oxidant to get higher yields. In order to overcome aforementioned drawbacks, new and improved catalysts for this reaction are still being sought. In designing such catalysts, special consideration should

be given to the cost and atom-economy of the particular catalytic processes. Additionally, the choice of solvent and catalyst should be made with the consideration of environmental impact in mind.

We began our studies by examining the cross-coupling of diphenyl diselenide **1** and 4-ethynyl toluene **2** as a model reaction to optimize experimental conditions and KO^tBu as a base in ethanol at 80 °C for 12 h under air. Without the aid of an additional catalyst, only 19% of **3** were observed by GC-MS analysis even after 24 h maintenance (Table 1, entry1). We found that the addition of 0.5 mol% of Fe₃O₄/C catalyst was found to offer 81% product yield after 12 h (Table 2, entry 2). Decreasing the basicity means increasing the recovery of starting materials (Table 1, entries 3-7) under identical conditions. It was also found that lowering the amount of base reduced the yield (71%) (Table 1, entry 8). Surprisingly, the prepared catalysts with different supports such as SBA-15 and graphene afforded 61% and 70% of corresponding cross-coupled products respectively; The mesoporous silica support SBA-15 is maybe not stable enough to completely stabilize Fe₃O₄ NPs, especially under a basic reaction condition with high temperatures. On the other hand, carbon supports like charcoal and graphene can be quite stable even under strong basic reactions. In table 1, both Fe₃O₄/C and Fe₃O₄/graphene showed high yields (70–71%) for the synthesis of alkynyl selenides via activation C-H and Se-Se bonds through a cross-coupling process based on their small particle sizes and high surface areas and robust frameworks of the support. Particularly, in terms of the efficiency against the support price, the Fe₃O₄/C catalyst among various carbon supported catalysts would be one of the best (The commercial price: single layer graphene=360\$ per 0.5g, activated charcoal=107\$ per 1000g). According to our knowledge, this is the first report to synthesize alkynyl selenides using ethanol as solvent in the absence of copper, ligands and additives with heterogeneous catalyst loading of 0.5 mol% of Fe₃O₄ NPs under environmentally benign conditions.

Based on the optimized reaction conditions, we then studied the scope of this novel system for a variety of substrates. As shown in Table 2, a wide range of aryl alkynes bearing electron-donating and electron-withdrawing were smoothly coupled with diphenyl diselenide, giving the corresponding alkynyl selenides in good to excellent yields (Table 2, entries 1-6). Aliphatic alkynes (1-ethynyl cyclohexene and 1-hexyne) were also successfully coupled with diaryl diselenides with 0.5% of Fe₃O₄ NPs/C (Table 2, entries 7 and 8). Similarly, diaryl diselenides with methoxy and trifluoromethyl groups were tolerated by Fe₃O₄ NPs catalyst (Table 2, entries 9 and 10).

Table 2. Evaluation of substrate scope

Entry	Alkyne	Product	Yield % ^[a]
1			91 (89) ^[b]
2			76
3			79
4			86
5			73
6			68
7			67 (61) ^[b]
8			81
9			100 (96) ^[b]
10			54

[a] Determined by GC-MS [b] Isolated yield, 12 h.

The catalyst could be recycled efficiently five times without significant loss of catalytic activity as clearly shown in Figure 4, confirming the high stability and robustness of the heterogeneous catalytic system. These findings are very important for expanding to organic processes in compliance with the principles of green chemistry and sustainability.

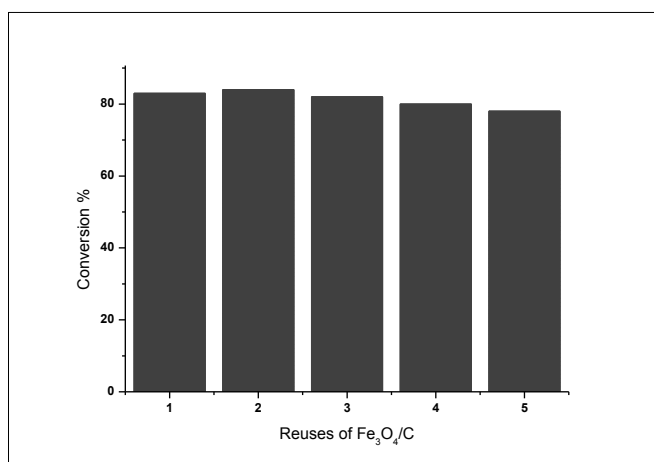


Figure 4. Recyclability of Fe₃O₄/C for the cross-coupling reaction of diphenyl diselenide and 4-ethynyl toluene

Conclusions

Magnetite nanoparticles on different solid supports (activated charcoal, graphene, and SBA-15), which were synthesized using the economically feasible solid-state grinding approach followed by a thermal treatment. The Fe₃O₄/C possesses a remarkable catalytic efficiency for the synthesis of alkynyl selenides via activation C-H and Se-Se bonds through a cross-coupling process. The porous charcoal based Fe₃O₄ catalyst could be reused more than five times, improving the high stability without prominent Fe leaching. The yields of target products with

challenged substituents were higher than traditional copper catalysts, highlighting the importance of nanocatalysts.

Experimental Section

Materials and methods

Chemicals Iron nitrate nonahydrate (Fe(NO₃)₃·9H₂O, ACS reagent, >98%) and activated charcoal (~100 mesh particle size, powder), Pluronic P123 (average Mn~5,800), tetraethoxysilane (TEOS, 98%), were purchased from Sigma-Aldrich. A single-layer graphene powder was obtained from ACS Material (USA). The chemicals were used as received without further purification.

Instrumentation ¹H NMR spectra were recorded on an Agilent 300 MHz spectrometer in the appropriate deuterated solvents. The chemical shift values were recorded as parts per million (ppm) relative to tetramethylsilane as an internal standard unless otherwise indicated, coupling constants are given in Hz. GC-MS spectra were recorded on a Shimadzu GC-MS Spectrometer. The nature of the magnetite nanoparticles was determined by using a powder X-ray diffractometer (Rigaku D/MAX-RB 12kW). The morphology of the catalysts was measured by using a Field emission Transmission Electron Microscope (Technai TF30 ST operated at 300 kV, KAIST). The surface areas for the catalysts were measured (samples were degassed in a vacuum at 300 °C for 4 h) by the Brunauer-Emmett-Teller (BET) method on a Tristar II 3020 at -196 °C.

Preparation of SBA-15 Mesoporous silica SBA-15 was prepared using a hydrothermal reaction according to the method reported in the literature.^[10] Typically, Pluronic P123 (16 g), distilled water (503 g), and HCl (97g) were added into a polypropylene bottle. The mixture was stirred until Pluronic P123 was completely dissolved in the acidic solution at room temperature. After that, TEOS (34 g) was added to the solution with stirring, and the mixture was aged at 40 °C for 24 h. After aging for 24 h, the mixture was transferred into a Teflon-lined autoclave and reacted at 150 °C for 24 h. The white powder was recovered through filtration, washed with water and ethanol thoroughly, and dried in air. The product was calcined at 550 °C for 5 h to produce SBA-15 with a pore diameter of 9.9 nm. The final calcined material had a surface area of 362 m²·g⁻¹ and a pore volume of 1.08 cm³·g⁻¹.

Preparation of Fe₃O₄/C, Fe₃O₄/SBA-15, and Fe₃O₄/graphene catalysts For the synthesis of Fe₃O₄/C, a mixture of Fe(NO₃)₃·9H₂O (0.29 g) and activated charcoal (0.5 g) in a mortar were physically ground until the color of the powder was homogeneously black. The mixture was transferred into a polypropylene bottle, and aged at 50 °C in a tumbling oven for 24 h. After that, the product was cooled under an ambient atmosphere and transferred to an alumina boat in a tube-type furnace. Finally, the Fe-incorporated charcoal powder was slowly heated at a ramping rate of 2.7 °C·min⁻¹ up to 350 °C under a nitrogen flow of 200 mL·min⁻¹. The sample was held at 350 °C for 4 h under a continuous nitrogen flow. For the preparation of the Fe₃O₄/SBA-15 and Fe₃O₄/graphene catalysts, all procedures were identical to the synthesis of Fe₃O₄/C, except for the use of 0.5 g of SBA-15 and single-layer graphene as a support, respectively.

Cross-coupling of alkyne and diphenyl diselenide In a typical reaction, diphenyl diselenide (100 mg, 0.32 mmol), phenyl acetylene (65 mg, 0.64 mmol), Fe₃O₄/C (3.7 mg, 0.5% with respect to diphenyl diselenide), base (72 mg, 0.64 mmol) and ethanol (2 mL) were added to an 10 mL aluminum capped vial and the mixture was stirred in a preheated oil bath maintained at 80 °C for 12 h. After maintenance, the Fe₃O₄ NPS were filtered through a celite bed and the product was extracted into diethyl ether. The organic solvent was evaporated by using a rotary evaporator. The residue was purified by column chromatography on silica gel with hexane as eluent to afford pure cross-coupled product. The CC reactions of other substrates were carried out in a similar way.

Acknowledgements

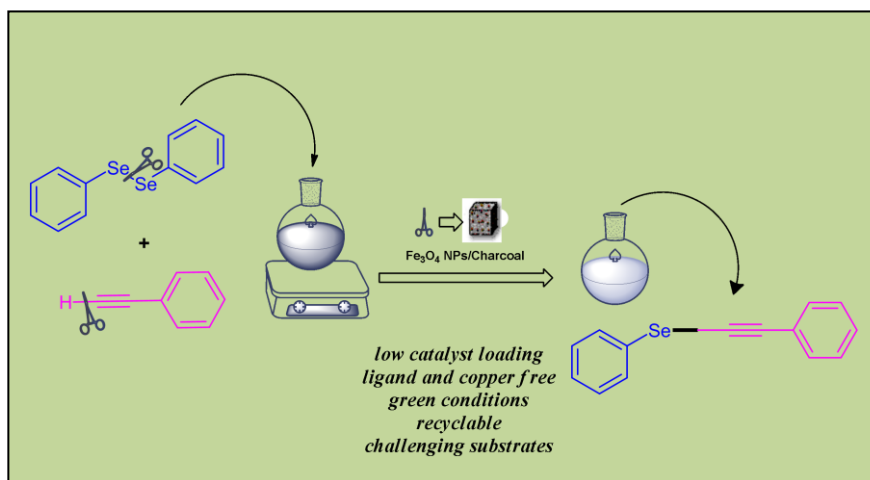
This research was supported by Basic Science Research Program through the National Research Foundation of Korea (NRF) funded by the Ministry of Science, ICT & Future Planning (NRF-2015R1D1A1A02060684 and NRF-2013R1A1A2012960).

Keywords: Alkynes • Diphenyl Diselenide • Iron-Oxide • Mechanochemistry • Nanocatalysts

- [1] a) A. Zhang, M. Liu, M. Liu, Y. Xiao, Z. Li, J. Chen, Y. Sun, J. Zhao, S. Fang, D. Jia, F. Li, *J. Mater. Chem. A* **2014**, *2*, 1369-1374. b) A. Zhang, Y. Tian, M. Liu, Y. Xiao, D. Jia, F. Li, *RSC Adv.* **2014**, *4*, 43973-43976. c) H. Wang, D. Wang, Z. peng, W. Tang, N. Li, F. Liu, *Chem. Commun.* **2013**, *49*, 5568-5570. d) E. Antolini, *ChemPlusChem* **2014**, *79*, 765-775. e) K. Zhang, F. Ren, H. Wang, C. Wang, M. Zhu, Y. Du, *ChemPlusChem* **2015**, *80*, 529-535. f) B. Mohan, H. Woo, S. Jang, S. Lee, S. Park, K. H. Park, *Solid State Sci.* **2013**, *22*, 16-20. g) N. Yan, C. Xiao, Y. Kou, *Coordination Chemistry Reviews* **2010**, *254*, 1179-1218.
- [2] a) T. Jin, M. Yan, Y. Yamamoto, *ChemCatChem* **2012**, *4*, 1217-1229. b) B. Mohan, C. Yoon, S. Jang, K. H. Park, *ChemCatChem* **2014**, *7*, 405-412. c) P. Zhao, X. Feng, D. Huang, G. Yang, D. Astruc, *Coordination Chemistry Reviews* **2015**, *287*, 114-136. d) A. Maximov, A. Zolotukhina, V. Murzin, E. Karakhanov, E. Rosenberg, *ChemCatChem* **2015**, *7*, 1197-1210. e) Y. Ma, Y. Huang, Y. Cheng, L. Wang, X. Li, *Appl. Catal. A* **2014**, *484*, 154-160. f) C. H. Campos, E. Rosenberg, J. L. G. Fierro, B. F. Urbano, B. L. Rivas, C. C. Torres, P. Reyes, *Appl. Catal. A* **2015**, *489*, 280-291. g) M. Zahmakrian, *Dalton Trans.* **2012**, *41*, 12690-12696. h) Z. Yinghui, K. Chenyan, A. T. Peng, A. Emi, W. Monalisa, L. K. Louis, N. S. Hosmane, J. A. Maguire, *Inorg. Chem.* **2008**, *47*, 5756-5761. i) K. Vijayakrishna, K. T. P. Charan, K. Manojkumar, S. Venkatesh, N. Pothanagandhi, A. Sivaramakrishna, P. Mayuri, A. Senthil Kumar, B. Sreedhar, *ChemCatChem* **2016**, *8*, 1-8. j) H. Inokawa, T. Ichikawa, H. Miyaoka, *Appl. Catal. A* **2015**, *491*, 184-188. k) V. Polshettiwar, C. Len, A. Fihri, *Coordination Chemistry Reviews* **2009**, *253*, 2599-2626. l) A. Chen, C. Ostrom, *Chem. Rev.* **2015**, *115*, 11999-12044.
- [3] a) C. W. Lim, I. S. Lee, *Nano Today* **2010**, *5*, 412-434. b) M. B. Gawande, P. S. Branco, R. S. Varma, *Chem. Soc. Rev.* **2013**, *42*, 3371. c) B. Karimi, F. Mansouri, H. M. Mirzaei, *ChemCatChem* **2015**, *7*, 1736-1789. d) C. Jin, Y. Wang, H. Wei, H. Tang, X. Liu, T. Lu, J. Wang, *J. Mater. Chem. A*, **2014**, *2*, 11202-11208.
- [4] a) L. Li, J. Lv, Y. Shen, X. Guo, L. Peng, Z. Xie, W. Ding, *ACS Catal.* **2014**, *4*, 2746-2752. b) J. Deng, L. P. Mo, F. Y. Zhao, Z. H. Zhang, S. X. Liu, *ACS Comb. Sci.* **2012**, *14*, 335-341. c) T. Zeng, W. W. Chen, C. M. Cirtiu, A. Moores, G. Song, C. J. Li, *Green Chem.* **2010**, *12*, 570-573. d) M. R. Nabid, Y. Bide, M. Niknezhad, *ChemCatChem* **2014**, *6*, 538-546. e) H. Firouzabadi, N. Iranpoor, M. Gholinejad, J. Hoseini, *Adv. Synth. Catal.* **2011**, *353*, 125-132. f) G. Yan, Y. Jiang, C. Kuang, S. Wang, H. Liu, Y. Zhang, J. Wang, *Chem. Commun.* **2010**, *46*, 3170-3172. g) S. Kim, E. Kim, B. M. Kim, *Chem. Asian J.* **2011**, *6*, 1921-1925.
- [5] a) G. Gorrasi, A. Sorrentino, *Green Chem.* **2015**, *17*, 2610-2625. b) E. Boldyreva, *Chem. Soc. Rev.* **2013**, *42*, 7719-7738. c) K. Ralphs, C. Hardacre, S. L. James, *Chem. Soc. Rev.* **2013**, *42*, 7701-7718. d) V. Safarifard, A. Morsali, *CrystEngComm*, **2012**, *14*, 5130-5132. e) L. Li, X. Guo, F. Hao, X. Zhang, J. Chen, *New J. Chem.* **2015**, *39*, 4731-4736.
- [6] a) G. Mugesh, W.W. Du Mont, H. Sies, *Chem. Rev.* **2001**, *101*, 2125-2180. b) C. W. Nogueira, G. Zeni, J. B. T. Rocha, *Chem. Rev.* **2004**, *104*, 6255-6286. c) V. Nascimento, N. L. Ferreira, R. F. S. Canto, K. L. Schott, E. P. Waczuk, L. Sancineto, C. Santi, J. B. T. Rocha, A. L. Braga, *Eur. J. Med. Chem.* **2014**, *87*, 131-139.
- [7] a) T. E. Frizon, J. Rafique, S. Saba, I. H. Bechtold, H. Gallardo, A. L. Braga, *Eur. J. Org. Chem.* **2015**, 3470-3476. b) A. Patra, Y. H. Wijsboom, G. Leitus, M. Bendikov, *Chem. Mater.* **2011**, *23*, 896-906. c) J. Gu, Z. A. Zhao, Y. Ding, H. L. Chen, Y. W. Zhang, C. H. Yan, *J. Am. Chem. Soc.* **2013**, *135*, 8363-8371. d) D. S. Rampon, F. S. Rodembusch, J. M. F. M. Schneider, I. H. Bechtold, P. F. B. Goncalves, A. A. Merlo, P. H. Schneider, *J. Mater. Chem.* **2010**, *20*, 715-722.
- [8] a) B. Mohan, S. Hwang, H. Woo, K. H. Park, *Synthesis* **2015**, *47*, 3741-3745. b) B. Mohan, S. Hwang, S. Jang, K. H. Park, *Synlett* **2014**, *25*, 2078-2082. c) B. Mohan, S. Hwang, H. Woo, K. H. Park, *Tetrahedron* **2014**, *70*, 2699-2702. d) B. Mohan, K. H. Park, *Appl. Catal. A* **2016**, *519*, 78-84.
- [9] a) E. Mohammadi, B. Movassagh, *Tetrahedron Lett.* **2014**, *55*, 1613-1615. b) A. Sharma, R. S. Schwab, A. L. Braga, T. Barcellos, M. W. Paixao, *Tetrahedron Lett.* **2008**, *49*, 5172-5174. c) L. W. Bieber, M. F. da Silva, P. H. Menezes, *Tetrahedron Lett.* **2004**, *45*, 2735-2737. d) M. Godoi, E. W. Ricardo, T. E. Frizon, M. S. T. Rocha, D. Singh, M. W. Paixao, A. L. Braga, *Tetrahedron* **2012**, *68*, 10426-10430. e) D. S. Rampon, R. Giovenardi, T. L. Silva, R. S. Rambo, A. A. Merlo, P. H. Schneider, *Eur. J. Org. Chem.* **2011**, 7066-7070. f) S. Ahammed, S. Bhadra, D. Kundu, B. Sreedhar, B. C. Ranu, *Tetrahedron* **2012**, *68*, 10542-10549.
- [10] H. R. Choi, H. Woo, S. Jang, J. Y. Cheon, C. Kim, J. Park, K. H. Park, S. H. Joo, *ChemCatChem* **2012**, *4*, 1587-1594.

Entry for the Table of Contents

COMMUNICATION



Balaji Mohan, Ji Chan Park*, Dr. Kang Hyun Park*

Page No. – Page No.

Mechanochemical Synthesis of Active Magnetite Nanoparticles Supported on Charcoal for Facile Synthesis of Alkynyl Selenides via C-H Activation